

## Incompressibility of polydisperse random-close-packed colloidal particles

Rei Kurita<sup>1</sup> and Eric R. Weeks<sup>2</sup>

<sup>1</sup>*Institute of Industrial Science, The University of Tokyo, 4-6-1 Komaba, Meguro-ku, Tokyo 153-8505, Japan*

<sup>2</sup>*Department of Physics, Emory University, Atlanta, Georgia 30322, USA*

(Received 9 July 2011; revised manuscript received 4 August 2011; published 12 September 2011)

We use confocal microscopy to study the compressibility of a random-close-packed sample of colloidal particles. To do this, we introduce an algorithm to estimate the size of each particle. Taking into account their sizes, we compute the compressibility of the sample as a function of wave vector  $q$ , and find that this compressibility vanishes linearly as  $q \rightarrow 0$ , showing that the packing structure is incompressible. The particle sizes must be considered to calculate the compressibility properly. These results also suggest that the experimental packing is hyperuniform.

DOI: [10.1103/PhysRevE.84.030401](https://doi.org/10.1103/PhysRevE.84.030401)

PACS number(s): 82.70.-y, 61.20.-p, 64.70.pv, 64.70.kj

The random packing of objects has been studied scientifically for nearly a century [1,2] (see Ref. [3] for a review). This problem is often termed random close packing (RCP) or maximally random jammed packing [4]. Important recent work has focused on the packing of highly polydisperse systems [5], ellipsoids [6], and tetrahedra [7], but the simplest packing problem is the packing of monodisperse spheres. In the past decade, simulations studying monodisperse spheres have generated large RCP configurations with  $10^5$ – $10^6$  spheres [8,9]. These simulations enable study of density fluctuations at very large length scales, or equivalently, small wave vectors  $q$ . They find that the static structure factor  $S(q)$  approaches zero linearly as  $q \rightarrow 0$ , that is,  $S(q) \sim q$  for small  $q$ . This finding has been termed hyperuniformity [10]. One corollary is that the sample is incompressible, as the isothermal compressibility  $\chi$  in simple liquids can be found from  $\rho k_B T \chi = S(0)$  where  $\rho$ ,  $k_B$ , and  $T$  are the mean density, Boltzmann constant, and temperature, respectively. These observations of close-packed samples are in contrast, for example, with simple liquids for which  $S(0) > 0$  [10,11]. The existence of hyperuniformity has been seen in a variety of systems (see for example discussions in Refs. [3,12]). In general, long wavelength density fluctuations are important for diverse fields including critical phenomena [13] and the shear flow of glassy materials [14]. Likewise, understanding random-close-packed samples is relevant for understanding liquids, glasses, biological systems, and granular materials [1,3,15]. The key connection between these two ideas was suggested in 2003 by Torquato and Stillinger, who conjectured that all close-packed samples should be hyperuniform given some reasonable ideas of what it means to be close packed [10].

In 2010 we published an experimental study of a random-close-packed sample of colloidal particles observed with confocal microscopy [16]. Our data set was the positions of more than 500 000 slightly polydisperse particles [17], and we found that  $S(q \rightarrow 0) > 0$ , implying that the experimental sample was compressible. A simulation of a binary sample found similar results [18]. These results seem to demonstrate random-close-packed samples that are not hyperuniform. However, two groups have shown that in polydisperse samples, careful consideration of the individual particle sizes recovers hyperuniformity and incompressibility [11,12]. In particular, Berthier *et al.* showed how to compute the isothermal

compressibility when the individual particle sizes are known, and demonstrated that samples with  $S(0) > 0$  nonetheless can be incompressible [11]. They examined data from a two-dimensional bidisperse granular experiment and confirmed that  $\chi(0) = 0$ . The reason  $S(0) > 0$  in polydisperse systems is because density fluctuations are coupled to composition fluctuations, but such samples can still be incompressible and hyperuniform.

In this Rapid Communication, our goal is to determine if our experimental sample is hyperuniform and incompressible. To do this, we first develop a method to determine each particle size from microscopy observations of a random-close-packed sample of colloidal particles. We use numerically generated packings to confirm that our method accurately determines the particle radii. Using these radii, we analyze our experimental data using the method of Berthier *et al.* [11]. Our results confirm that our experimental system is hyperuniform and incompressible. In contrast to the experimental data of Ref. [11] (a two-dimensional bidisperse sample), we study a three-dimensional sample with a continuous distribution of sizes.

As we use the analytical method introduced by Berthier *et al.* [11], we briefly summarize their method here. They consider a wave-vector-dependent isothermal compressibility  $\chi(q)$ , which is related to the structure factor of a monodisperse sample by  $\rho k_B T \chi(q) = S(q)$ . They then derive an exact formula relating  $\chi(q)$  and  $S(q)$  for a polydisperse sample, although the formula is “conceptually and computationally difficult” to evaluate [11]. Thus, they derive a series of approximate formulas, of which the first-order approximation is sufficient for samples of low polydispersity such as ours. To start with, they define single-particle density fields  $\rho_i(\mathbf{q}) = \exp(i\mathbf{q} \cdot \mathbf{r}_i)$  where  $\mathbf{r}_i$  is the position of particle  $i$ . They also define the size deviation of particle  $i$  as  $\epsilon_i = (a_i - \bar{a})/\bar{a}$ , where  $a_i$  is the radius of particle  $i$  and  $\bar{a}$  is the mean radius. (Note that  $\sqrt{\langle \epsilon_i^2 \rangle} = p$  defines the polydispersity  $p$  of a sample.) These  $\epsilon_i$  are the small parameters used in the approximation. Using these variables, they define a  $2 \times 2$  matrix  $S(q)$  with elements  $S^{uv}(q) = \frac{1}{N} \langle \epsilon^u(\mathbf{q}) \epsilon^v(-\mathbf{q}) \rangle$ , with  $u, v \in 0, 1$ ,  $\epsilon^0(q) = \sum_{i=1}^N \epsilon_i^0 \rho_i(q)$ , and  $N$  is the total number of particles. The matrix elements can be used to provide a first-order approximation  $\chi_1(q)$  as  $\rho k_B T \chi_1(q) = S^{00} - [S^{01}]^2 / S^{11}$ . They confirm that  $\chi_1(0) \approx 0$  in cases for which the sample polydispersity is less

than 10%, while  $S(0) \neq 0$  for those cases. Their results suggest that random-close-packed systems are hyperuniform and incompressible even when the sample is polydisperse [11,12]. It is important to note that strictly speaking, the relationship between structure and compressibility is a thermodynamic one and thus it assumes the sample is equilibrium, which a random-close-packed sample certainly violates. However, Ref. [11] is a good demonstration that this condition is not crucial.

In our prior work, we used colloidal particles to generate a random-close-packed sample, and imaged this with confocal microscopy. We reprise the key experimental points here; a more detailed experimental discussion is in Ref. [16]. We use sterically stabilized poly(methyl methacrylate) (PMMA) particles with  $\bar{a} = 1.265 \mu\text{m}$ . Previously we reported that these particles had a polydispersity of  $\sim 5\%$  [16]; below, we determine that the true polydispersity is 6.7%. The PMMA particles are suspended in a solvent mixture that is slightly lower density than the particles. The sample is mixed and then the particles are allowed to sediment until they are close packed. We use a confocal microscope to take clear images deep inside our dense sample [19]. Overlapping images are taken, with total volume  $492 \times 514 \times 28 \mu\text{m}^3$ . Within this volume, particles are identified within  $0.03 \mu\text{m}$  in  $x$  and  $y$ , and within  $0.05 \mu\text{m}$  in  $z$  [19,20]. The total data set contains 543 136 particles [17].

*Estimating particle radii.* The average particle size  $\bar{a}$  is obtained from the position of the first peak of the pair correlation function [16]. It is difficult to determine subtle size differences between individual particles from microscopy due to diffraction. However, obtaining the positions of each particle can be done accurately. A large particle will be slightly farther from its neighbors as compared to a small particle, and we use this idea as a starting point for an estimation method for each particle size.

Given that our sample is jammed, each particle must be in contact with several of its neighbors. In fact, a numerical simulation of random-close-packed monodisperse particles showed that the mean contact number is 6 [10]. When particle  $i$  contacts with particle  $j$ , the separation between these two particles is given by  $r_{ij} = a_i + a_j$ , where  $a_i$  and  $a_j$  are their radii. The average of  $r_{ij}$  over all neighbors  $j$  is given by  $\langle r_{ij} \rangle_j = a_i + \langle a_j \rangle_j$ . Next, consider separations  $r_{jk}$  between particle  $i$ 's contacting neighbors  $j$  and contacting neighbors  $k$  of those particles. Again, we take an average of  $r_{jk}$  with respect to particles  $j$  and  $k$ , giving  $\langle \langle r_{jk} \rangle_k \rangle_j = \langle a_j \rangle_j + \langle \langle a_k \rangle_k \rangle_j$ . Then we subtract  $\langle \langle r_{jk} \rangle_k \rangle_j$  from  $\langle r_{ij} \rangle_j$ , leading to

$$a_i = \langle \langle a_k \rangle_k \rangle_j + \langle r_{ij} \rangle_j - \langle \langle r_{jk} \rangle_k \rangle_j. \quad (1)$$

In practice, we choose the  $Z = 5$  nearest-neighbor particles from particle  $i$  as the particles  $j$ , and assume these are the contacting particles. Likewise for each particle  $j$  we identify its  $Z$  closest neighbors for the particles  $k$ . The choice  $Z = 5$  is justified below. To compute  $\langle \langle a_k \rangle_k \rangle_j$ , we use  $\bar{a}$  as an initial guess for the particle sizes, and then iterate five times to get more accurate values for  $a_i$ . In this way  $a_i$  is found from the particle separations, which are obtained directly from microscopy.

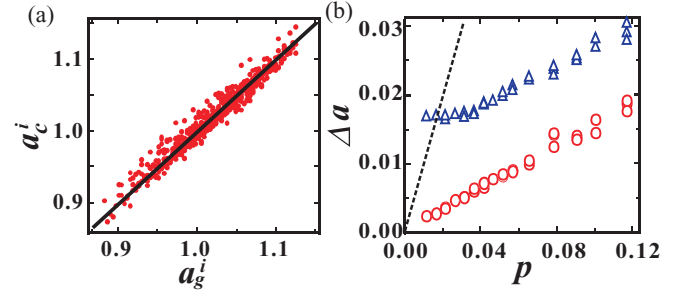


FIG. 1. (Color online) (a) Scatter plot of the calculated radius  $a_c^i$  from our method [Eq. (1)] as a function of the given radius  $a_g^i$  using data from a simulated packing with polydispersity 7%. The solid line corresponds to  $a_c^i = a_g^i$ . (b) The particle size uncertainty  $\Delta a$  found by analyzing simulation data from packings with a given polydispersity, both without noise (circles) and with noise added to the particle positions (triangles). The dashed line corresponds  $\Delta a = p$ .

To validate our method, we simulate polydisperse RCP samples using the algorithm of Refs. [21,22]. We use 512 particles with mean radius  $\bar{a} = 1$  and polydispersity from 0.01 to 0.12, generating five independent configurations for each polydispersity. The particle size distribution is a Gaussian. Using the simulated position centers, we calculate the radii of the particles  $a_c^i$  by our method. Figure 1(a) shows a scatter plot of  $a_c^i$  as a function of the given radii  $a_g^i$  from a simulation with 7% polydispersity. The calculated radii are located around  $a_c^i = a_g^i$ . We define the uncertainty of the size estimation as  $\Delta a = \sqrt{\langle [(a_c^i - a_g^i)/a_g^i]^2 \rangle_i}$ .  $\Delta a$  is plotted as a function of polydispersity  $p$  as circles in Fig. 1(b). We find  $\Delta a \approx p/6$ . The polydispersity of  $a_c^i$  matches that of  $a_g^i$ .

One experimental complication is that there is an uncertainty in the position of each particle. In our experiment, the uncertainties are  $0.024\bar{a}$  in  $x$  and  $y$  and  $0.0395\bar{a}$  in  $z$ . We add this positional uncertainty to the true simulated positions, and then redetermine the particle radii. As expected, this increases the uncertainty  $\Delta a$  of the final radii, shown by the triangles in Fig. 1(b).  $\Delta a$  increases by  $\sim 0.01$  compared to the case without positional noise. Positional noise is fatal when the

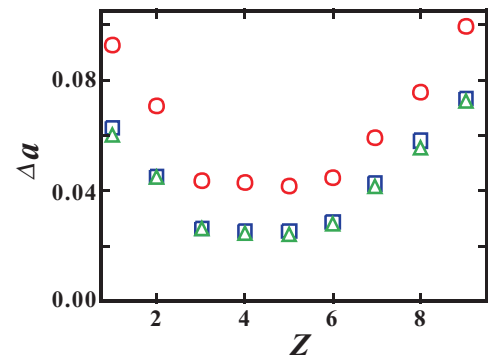


FIG. 2. (Color online) The uncertainty of the particle radius  $\Delta a$  is plotted as a function of the number of contacting neighbors  $Z$  used in the algorithm. The data are from the simulated packings with a polydispersity  $p = 0.07$  with positional noise. Circles correspond to Eq. (1) using  $\langle \langle a_k \rangle_k \rangle_j = \bar{a}$  with no iteration. Squares correspond to five iterations of Eq. (1), and triangles correspond to ten iterations.

polydispersity is less than 0.02, but otherwise our method results in more accurate radii even in the presence of noise.

While the mean contact number for particles at jamming should be 6, this contact number fluctuates from particle to particle. Thus our choice of a fixed  $Z = 5$  introduces some noise. Revising our method to allow  $Z$  to vary from particle to particle decreases  $\Delta a$  only slightly at best. At worst, this is quite sensitive to how contacts are defined, and  $\Delta a$  can be larger than the case with fixed  $Z$ . We justify our choice of  $Z = 5$  from the data shown in Fig. 2. The square symbols show how  $\Delta a$  depends on  $Z$  for five iterations of Eq. (1), and the data have a minimum at  $Z = 5$  although it is apparent that  $Z = 3, 4$ , and 6 work almost as well. Figure 2 also demonstrates that five iterations (squares) is essentially as good as ten iterations (triangles).

Next, we estimate each particle size of our experimental data with our method. Given that Eq. (1) requires information about both a particle's nearest neighbors and also second nearest neighbors, only particles sufficiently far from the edges of our images have accurate sizes. We modify our algorithm slightly for the experimental data as follows. We find the coordination number  $z_i$  of each particle, the number of neighboring particles within a distance  $2.8a$  (the first minimum of the pair correlation function) [16]. From the particles in the interior of the sample, we find the average coordination number  $\bar{z} \approx 12$ . Then, for every particle, we estimate the number of touching neighbors  $T_i = 5z_i/12$  where we round  $T_i$  to the nearest integer. For particles at the edge of the imaged volume,  $T_i < 5$  as not all of the neighbors are imaged. Then for each particle, when averages over contacting neighbors  $j$  are done in Eq. (1), these averages are over the  $T_i$  nearest neighbors. After iterating Eq. (1) to find all radii, the edge particles are removed by cropping the data to a volume of  $440 \times 461 \times 14.2 \mu\text{m}^3$ , containing 217 816 particles.

Based on these particles with their calculated sizes, the volume fraction of this sample is found to be  $\phi = 0.647 \pm 0.007$ , where the uncertainty of  $\phi$  is due to the uncertainty in determination of each particle size. Figure 3 shows a distribution of the estimated particle sizes. This sample has a polydispersity of 6.7%.<sup>1</sup> Given this measured polydispersity, Fig. 1(b) shows that  $\Delta a \approx 0.023$  (corresponding to  $\bar{a}\Delta a = 0.03 \mu\text{m}$ ). The experimental distribution is not a Gaussian and this is not an artifact of our method, as a simulated Gaussian size distribution with positional noise leads to a measured Gaussian size distribution.

*Compressibility of experimental packing.* Using our estimated particle sizes, we now study the wave vector dependence of the compressibility  $\chi_0(q)$  and  $\chi_1(q)$  of our experimental data. Given the aspect ratio of our box, which is thin in

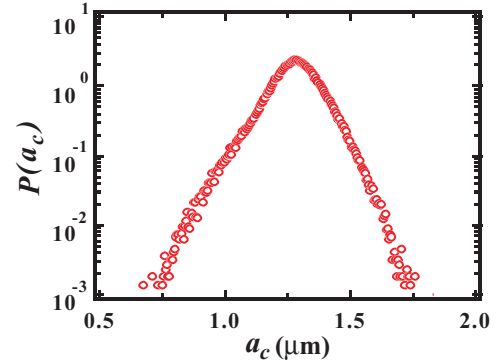


FIG. 3. (Color online) Probability of particle sizes in our experimental sample. The average size is  $1.265 \mu\text{m}$  and polydispersity is 6.7%.

the  $z$  direction, we compute the Fourier transforms using wave vectors in the  $q_x q_y$  plane. Figure 4 shows  $\rho k_B T \chi_0(q)$  and  $\rho k_B T \chi_1(q)$ . Our experimental data do not obey periodic boundary conditions, and the effect of the boundaries appears near  $q = 0$ . We calculate  $\chi_0(q)$  and  $\chi_1(q)$  with a variety of window functions, and the fluctuations due to these different choices are indicated by the error bars in Fig. 4.  $\chi_0(q)$  and  $\chi_1(q)$  are independent of the choice of Fourier window functions for  $q\bar{a}/\pi > 0.2$ . For  $q\bar{a}/\pi > 0.5$ , an upward curvature is seen as the first peak of  $S(k)$  is approached; this curvature starting at  $q\bar{a}/\pi \approx 0.5$  is also seen in simulations with

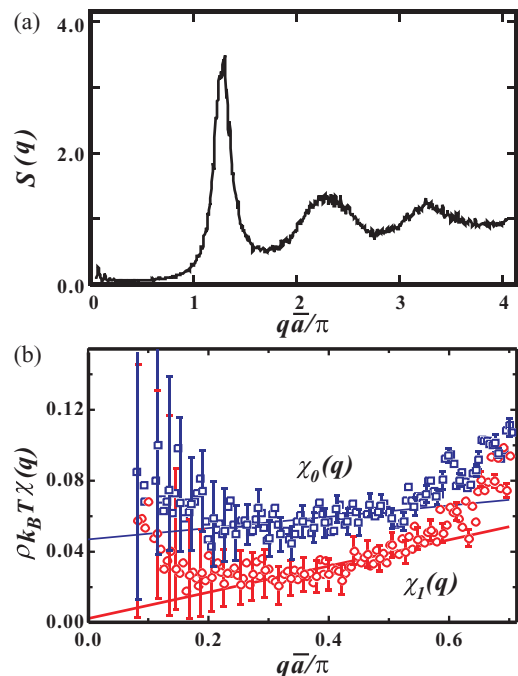


FIG. 4. (Color online) (a) The static structure factor  $S(q)$ . (b)  $\rho k_B T \chi_0(q)$  (no approximation) and  $\rho k_B T \chi_1(q)$  (first-order approximation of Ref. [11]), from the experimental data. Square symbols correspond to  $\rho k_B T \chi_0(q)$ , which is proportional to  $S(q)$  at small  $q$ . Circle symbols correspond to  $\rho k_B T \chi_1(q)$ . The error bars (drawn for every fifth point) are from using different windowing functions in the Fourier transform. The lines are linear fits to the data for  $0.2 < q\bar{a}/\pi < 0.5$ .

<sup>1</sup>The measured polydispersity of our sample (6.7%) helps explain a discrepancy we previously noted between our observations [16] and those of Dullens *et al.*, who also studied dense suspensions of sedimenting particles [24]. Their particles formed crystals during the sedimentation, while our particles pack randomly. Their samples had a polydispersity of 5%, while the polydispersity of our sample is 6.7%. Crystal nucleation is sensitive to polydispersity in this range [23] and this likely explains why our sample avoids crystallization, and why the samples of Dullens *et al.* crystallized.

$10^6$  particles [8]. Thus we do a linear fit to  $\rho k_B T \chi_0(q)$  and  $\rho k_B T \chi_1(q)$  in the region  $0.2 < q\bar{a}/\pi < 0.5$ , shown as the lines in Fig. 4. Both functions have linear behavior in this region, and this is the same region fit in Ref. [16]. We find  $\rho k_B T \chi_1(0) = 0.002 \pm 0.004$ , while  $\rho k_B T \chi_0(0) = 0.049 \pm 0.008$  as reported previously [16]. The uncertainties are due to the uncertainties of particle positions and sizes, and the choice of the fitting range. Our observation that  $\chi_1(q) \sim q$  shows that long wavelength density fluctuations are suppressed. This is consistent with the observations of Berthier *et al.* and shows that our system is incompressible [11]. To be clear, we are neglecting the solvent, so technically we are demonstrating that if we place hard spheres with the estimated sizes at the locations we measure from the colloidal sample, the hard sphere system will be incompressible.

To summarize, we have presented a method to estimate the sizes of individual colloidal particles from experimental knowledge of only their positions, and relying on the fact that the sample is close packed. Numerical simulations confirm that our method is robust even in the presence of realistic experimental noise. Using the positions and sizes of over 200 000 random-close-packed particles from our experiment, we confirm that our experimental system is hyperuniform and incompressible. Our results are consistent with prior work [11,12] and the data can be used with other algorithms for quantifying hyperuniformity in polydisperse samples [12].

E.R.W. was supported by the National Science Foundation (Grant No. CHE-0910707). We thank K. Schweizer and S. Torquato for helpful discussions.

- 
- [1] W. O. Smith, P. D. Foote, and P. F. Busang, *Phys. Rev.* **34**, 1271 (1929).
  - [2] A. E. R. Westman and H. R. Hugill, *J. Am. Ceram. Soc.* **13**, 767 (1930).
  - [3] S. Torquato and F. H. Stillinger, *Rev. Mod. Phys.* **82**, 2633 (2010).
  - [4] S. Torquato, T. M. Truskett, and P. G. Debenedetti, *Phys. Rev. Lett.* **84**, 2064 (2000).
  - [5] M. Clusel, E. I. Corwin, A. O. N. Siemens, and J. Brujic, *Nature (London)* **460**, 611 (2009).
  - [6] A. Donev *et al.*, *Science* **303**, 990 (2004).
  - [7] E. Chen, M. Engel, and S. Glotzer, *Discrete and Computational Geometry* **44**, 253 (2010).
  - [8] A. Donev, F. H. Stillinger, and S. Torquato, *Phys. Rev. Lett.* **95**, 090604 (2005).
  - [9] L. E. Silbert and M. Silbert, *Phys. Rev. E* **80**, 041304 (2009).
  - [10] S. Torquato and F. H. Stillinger, *Phys. Rev. E* **68**, 041113 (2003); **68**, 069901 (2003).
  - [11] L. Berthier, P. Chaudhuri, C. Coulais, O. Dauchot, and P. Sollich, *Phys. Rev. Lett.* **106**, 120601 (2011).
  - [12] C. E. Zachary, Y. Jiao, and S. Torquato, *Phys. Rev. Lett.* **106**, 178001 (2011); *Phys. Rev. E* **83**, 051308 (2011); **83**, 051309 (2011).
  - [13] A. Onuki, *Phase Transition Dynamics* (Cambridge University Press, Cambridge, 2002).
  - [14] A. Furukawa and H. Tanaka, *Nature Mater.* **8**, 601 (2009).
  - [15] J. D. Bernal and J. Mason, *Nature (London)* **188**, 910 (1960).
  - [16] R. Kurita and E. R. Weeks, *Phys. Rev. E* **82**, 011403 (2010).
  - [17] See Supplemental Material at <http://link.aps.org/supplemental/10.1103/PhysRevE.82.011403> for a file of the particle coordinates.
  - [18] N. Xu and E. S. C. Ching, *Soft Matter* **6**, 2944 (2010).
  - [19] A. D. Dinsmore, E. R. Weeks, V. Prasad, A. C. Levitt, and D. A. Weitz, *Appl. Opt.* **40**, 4152 (2001).
  - [20] J. C. Crocker and D. G. Grier, *J. Colloid Interface Sci.* **179**, 298 (1996).
  - [21] N. Xu, J. Blawdziewicz, and C. S. O'Hern, *Phys. Rev. E* **71**, 061306 (2005).
  - [22] K. W. Desmond and E. R. Weeks, *Phys. Rev. E* **80**, 051305 (2009).
  - [23] S. Auer and D. Frenkel, *Nature (London)* **413**, 711 (2001).
  - [24] R. P. A. Dullens, D. G. A. L. Aarts and W. K. Kegel, *Phys. Rev. Lett.* **97**, 228301 (2006).